VIETNAM ACADEMY OF SCIENCE AND TECHNOLOGY

Vietnam Journal of MECHANICS

Volume 36 Number 1

ISSN 0866-7136

VN INDEX 12.666

1

2014

Vietnam Journal of Mechanics, VAST, Vol. 36, No. 1 (2014), pp. 27 – 47

NONLINEAR STATIC AND DYNAMIC BUCKLING OF ECCENTRICALLY STIFFENED FUNCTIONALLY GRADED CYLINDRICAL SHELLS UNDER AXIAL COMPRESSION SURROUNDED BY AN ELASTIC FOUNDATION

Vu Hoai Nam[1,*], **Nguyen Thi Phuong**[1], **Dao Huy Bich**[2], **Dao Van Dung**[2]
[1] *University of Transport Technology, Hanoi, Vietnam*
[2] *Hanoi University of Science, VNU, Vietnam*
[*]E-mail: hoainam.vu@utt.edu.vn
Received November 06, 2013

Abstract. This paper presents an analytical approach to investigate the nonlinear buckling of imperfect eccentrically stiffened functionally graded thin circular cylindrical shells subjected to axial compression and surrounded by an elastic foundation. Based on the classical thin shell theory with the geometrical nonlinearity in von Karman-Donnell sense, initial geometrical imperfection, the smeared stiffeners technique and Pasternak's two-parameter elastic foundation, the governing equations of eccentrically stiffened functionally graded cylindrical shells are derived. The functionally graded cylindrical shells are reinforced by homogeneous ring and stringer stiffener system on internal and (or) external surface. The resulting equations are solved by the Galerkin method to obtain the explicit expression of static critical buckling load, post-buckling load-deflection curve and nonlinear dynamic motion equation. The nonlinear dynamic responses are found by using fourth order Runge-Kutta method. The dynamic critical buckling loads of shells are considered for step loading of infinite duration and linear-time compression. The obtained results show the effects of foundation, stiffeners and input factors on the nonlinear buckling behavior of these structures.

Keywords: Static and dynamic buckling analysis, elastic foundation, stiffener, functionally graded material, stiffened circular cylindrical shell, critical buckling load.

1. INTRODUCTION

In recent years, the mechanic behavior of functionally graded (FGM) cylindrical shell attracts special attention of many authors. In static buckling analysis of FGM cylindrical shells without elastic foundation, many studies have been focused on the buckling and post-buckling of shells under mechanic and thermal loading. Shen [1–3] and Shen and Noda [4] presented the nonlinear postbuckling of perfect and imperfect FGM cylindrical thin shells under axial compression, radial pressure and combined axial and radial loads. Huang and Han [5–9] studied the buckling and postbuckling of un-stiffened FGM cylindrical shells

under torsion load, axial compression, radial pressure, combined axial compression and radial pressure based on the Donnell shell theory and the nonlinear strain-displacement relations of large deformation. Shen [10] investigated the torsional buckling and postbuckling of FGM cylindrical shells in thermal environments. The non-linear static buckling of FGM conical shells which is more general than cylindrical shells, were studied by Sofiyev [11, 12]. Zozulya and Zhang [13] studied the behavior of functionally graded axisymmetric cylindrical shells based on the high order theory.

For dynamic buckling analysis of FGM cylindrical shells without elastic foundation, Darabi et al. [14] presented respectively linear and nonlinear parametric resonance analyses for un-stiffened FGM cylindrical shells. Sofiyev and Schnack [15] and Sofiyev [16] obtained critical parameters for un-stiffened cylindrical thin shells under linearly increasing dynamic torsional loading and under a periodic axial impulsive loading by using the Galerkin technique together with Ritz type variation method. Sheng and Wang [17] presented the thermo-mechanical vibration analysis of FGM shell with flowing fluid. Sofiyev [18–21] and Deniz and Sofiyev [22] were investigated the vibration and dynamic instability of FGM conical shells. Hong [23] studied thermal vibration of magnetostrictive FGM cylindrical shells. Huang and Han [24] presented the nonlinear dynamic buckling problems of un-stiffened functionally graded cylindrical shells subjected to time-dependent axial load by using the Budiansky-Roth dynamic buckling criterion [25]. Various effects of the inhomogeneous parameter, loading speed, dimension parameters; environmental temperature rise and initial geometrical imperfection on nonlinear dynamic buckling were discussed.

For FGM cylindrical shell surrounded by an elastic foundation, the postbuckling of shear deformable FGM cylindrical shells surrounded by an elastic medium was studied by Shen [26]. Shen et al. [27] investigated postbuckling of internal pressure loaded FGM cylindrical shells surrounded by an elastic medium. Bagherizadeh et al. [28] investigated mechanical buckling of FGM cylindrical shells surrounded by Pasternak's elastic foundation. Sofiyev [29] analyzed the buckling of FGM circular shells under combined loads and resting on the Pasternak's elastic foundation. Torsional vibration and stability of functionally graded orthotropic cylindrical shells on elastic foundations is presented by Najafov et al. [30]. For the FGM conical shell-general case of FGM cylindrical shells, mechanic behavior of shell on elastic foundation was studied in [31–33].

In engineering structures, the reinforcement by stiffener system provides the benefit of added load carrying capability with a relatively small additional weight. Thus study on nonlinear static and dynamic behavior of theses structures are significant practical problem. However, up to date, the investigation on this field has received comparatively little attention. Recently, Najafizadeh et al. [34] have studied linear static buckling of FGM axially loaded cylindrical shell reinforced by ring and stringer FGM stiffeners. Bich et al. [35–38] have investigated the nonlinear static and dynamic analysis of FGM plates, cylindrical panels, shallow shells and circular cylindrical shells with eccentrically homogeneous stiffener system. Dung and Hoa [39, 40] presented an analytical study of nonlinear static buckling and post-buckling analysis of eccentrically stiffened functionally graded circular cylindrical shells under external pressure and torsional load with FGM stiffeners and approximate three-term solution of deflection taking into account the nonlinear buckling

shape. Dung et al. [41] studied the instability of eccentrically stiffened functionally graded truncated conical shells under mechanical loads.

This paper investigates the nonlinear behavior of ES-FGM cylindrical shells surrounded by an elastic foundation by an analytical approach. The nonlinear governing equations of eccentrically stiffened FGM circular cylindrical shells surrounded by an elastic foundation are derived based on the classical shell theory with the nonlinear strain-displacement relation of large deflection, the smeared stiffeners technique and two-parameter elastic foundation Pasternak. By using the Galerkin method, the closed-form relation of static critical buckling load and load-deflection postbuckling curves are obtained. Numerical nonlinear dynamic responses are found from Runge-Kutta method. The dynamic buckling loads of shells under step loading of infinite duration are found correspondingly to the load value of sudden jump in the average deflection and those of shells under linear-time compression are investigated according to Budiansky-Roth criterion. The results show that the foundation, stiffener, volume-fractions index and initial imperfection strongly influence to the behavior of shells.

2. ECCENTRICALLY STIFFENED FGM (ES-FGM) CIRCULAR CYLINDRICAL SHELLS SURROUNDED BY AN ELASTIC FOUNDATION

2.1. Functionally graded material

By applying a simple power law distribution, the volume fractions of metal and ceramic are obtained as follows

$$V_m + V_c = 1,$$

$$V_c = V_c(z) = \left(\frac{2z+h}{2h}\right)^k,$$

where h is thickness of shell; $k \geq 0$ is volume-fraction index; z is thickness coordinate and varies from $-h/2$ to $h/2$; the subscripts m and c refer to metal and ceramic constituents respectively. According to the mentioned law, Young modulus and mass density can be obtained in expressions

$$\begin{aligned} E(z) &= E_m V_m + E_c V_c = E_m + (E_c - E_m)\left(\frac{2z+h}{2h}\right)^k, \\ \rho(z) &= \rho_m V_m + \rho_c V_c = \rho_m + (\rho_c - \rho_m)\left(\frac{2z+h}{2h}\right)^k, \end{aligned} \tag{1}$$

Poissons's ratio ν is assumed to be constant.

2.2. Governing equations

Consider a FGM thin circular cylindrical shell with length L, mean radius R (Fig. 1). This shell is assumed to be reinforced by closely spaced (Najafizadeh et al. [34]; Brush and Almroth [42]; Reddy and Starnes [43]) homogeneous ring and stringer stiffener systems (see Fig. 1). The shell is surrounded by a Pasternak's two-parameter elastic foundation with

K_1 (N/m^3) is Winkler foundation modulus and K_2 (N/m) is the shear layer foundation stiffness of Pasternak model.

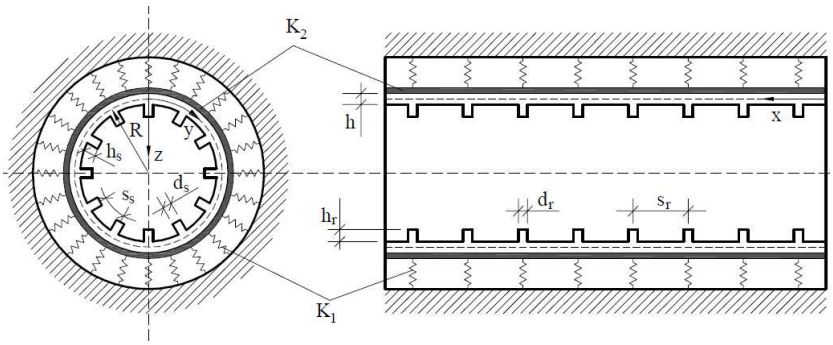

Fig. 1. Geometry and coordinate system of an eccentrically stiffened cylindrical shell surrounded by an elastic foundation

The origin of coordinate locates on the middle plane and at the left end of the shell, x, y ($y = R\theta$) and z axes are in the axial, circumferential, and inward radial directions, respectively.

This paper assume that stiffener is pure-ceramic if it is located at ceramic-rich side and is pure-metal if is located at metal-rich side, such FGM stiffened circular cylindrical shells provide continuity within shell and stiffeners and can be easier manufactured. Based the von Karman nonlinear strain-displacement relations (Brush and Almroth [42]), the strain components at the middle plane of shells are obtained by

$$\begin{aligned}
\varepsilon_x^0 &= \frac{\partial u}{\partial x} + \frac{1}{2}\left(\frac{\partial w}{\partial x}\right)^2 + \frac{\partial w}{\partial x}\frac{\partial w_0}{\partial x},\\
\varepsilon_y^0 &= \frac{\partial v}{\partial y} - \frac{w}{R} + \frac{1}{2}\left(\frac{\partial w}{\partial y}\right)^2 + \frac{\partial w}{\partial y}\frac{\partial w_0}{\partial y},\\
\gamma_{xy}^0 &= \frac{\partial u}{\partial y} + \frac{\partial v}{\partial x} + \frac{\partial w}{\partial x}\frac{\partial w}{\partial y} + \frac{\partial w}{\partial y}\frac{\partial w_0}{\partial x} + \frac{\partial w}{\partial x}\frac{\partial w_0}{\partial y},\\
\chi_x &= \frac{\partial^2 w}{\partial x^2}, \chi_y = \frac{\partial^2 w}{\partial y^2}, \chi_{xy} = \frac{\partial^2 w}{\partial x \partial y},
\end{aligned} \tag{2}$$

where $u = u(x, y)$, $v = v(x, y)$ and $w = w(x, y)$ are displacements along x, y and z axes, respectively, and χ_x, χ_y, χ_{xy} are the changes of curvatures and twist of shell, respectively, and $w_0 = w_0(x, y)$ denotes initial imperfection of shell, which is very small compared with the shell dimensions, but may be compared with the shell wall thickness. The strains across the shell thickness at a distance z from the mid-surface are given by

$$\begin{aligned}
\varepsilon_x &= \varepsilon_x^0 - z\chi_x,\\
\varepsilon_y &= \varepsilon_y^0 - z\chi_y,\\
\gamma_{xy} &= \gamma_{xy}^0 - 2z\chi_{xy}.
\end{aligned} \tag{3}$$

From Eq. (2) the strains must be relative in the deformation compatibility equation

$$\frac{\partial^2 \varepsilon_x^0}{\partial y^2} + \frac{\partial^2 \varepsilon_y^0}{\partial x^2} - \frac{\partial^2 \gamma_{xy}^0}{\partial x \partial y} = -\frac{1}{R}\frac{\partial^2 w}{\partial x^2} + \left(\frac{\partial^2 w}{\partial x \partial y} + \frac{\partial^2 w_0}{\partial x \partial y}\right)^2 - \\ - \left(\frac{\partial^2 w}{\partial x^2} + \frac{\partial^2 w_0}{\partial x^2}\right)\left(\frac{\partial^2 w}{\partial y^2} + \frac{\partial^2 w_0}{\partial y^2}\right). \tag{4}$$

Hooke's stress-strain relation is applied for the shell

$$\sigma_x^{sh} = \frac{E(z)}{1-\nu^2}\left(\varepsilon_x + \nu\varepsilon_y\right), \quad \sigma_y^{sh} = \frac{E(z)}{1-\nu^2}\left(\varepsilon_y + \nu\varepsilon_x\right), \quad \tau_{xy}^{sh} = \frac{E(z)}{2\left(1+\nu\right)}\gamma_{xy}, \tag{5}$$

and for stiffeners

$$\sigma_x^s = E_s\varepsilon_x, \quad \sigma_y^r = E_r\varepsilon_y, \tag{6}$$

where E_s, E_r are Young's modulus of stringer and ring stiffeners, respectively.

The force and moment of an un-stiffened FGM circular cylindrical shell can be determined by

$$\left\{\left(N_x, N_y, N_{xy}\right), \left(M_x, M_y, M_{xy}\right)\right\} = \int_{-h/2}^{h/2} \left\{\sigma_x, \sigma_y, \sigma_{xy}\right\}\left(1, z\right) \mathrm{d}z. \tag{7}$$

According to the smeared stiffeners technique and omitting the twist of stiffeners, the expressions for force and moment resultants are expressed in the form

$$\begin{aligned} N_x &= \left(A_{11} + \frac{E_s A_s}{s_s}\right)\varepsilon_x^0 + A_{12}\varepsilon_y^0 - \left(B_{11} + C_s\right)\chi_x - B_{12}\chi_y, \\ N_y &= A_{12}\varepsilon_x^0 + \left(A_{22} + \frac{E_r A_r}{s_r}\right)\varepsilon_y^0 - B_{12}\chi_x - \left(B_{22} + C_r\right)\chi_y, \\ N_{xy} &= A_{66}\gamma_{xy}^0 - 2B_{66}\chi_{xy}, \end{aligned} \tag{8}$$

$$\begin{aligned} M_x &= \left(B_{11} + C_s\right)\varepsilon_x^0 + B_{12}\varepsilon_y^0 - \left(D_{11} + \frac{E_s I_s}{s_s}\right)\chi_x - D_{12}\chi_y, \\ M_y &= B_{12}\varepsilon_x^0 + \left(B_{22} + C_r\right)\varepsilon_y^0 - D_{12}\chi_x - \left(D_{22} + \frac{E_r I_r}{s_r}\right)\chi_y, \\ M_{xy} &= B_{66}\gamma_{xy}^0 - 2D_{66}\chi_{xy}, \end{aligned} \tag{9}$$

where $A_{ij}, B_{ij}, D_{ij}\,(i,j = 1,2,6)$ are extensional, coupling and bending stiffness of the un-stiffened FGM cylindrical shell,

$$\begin{aligned} A_{11} &= A_{22} = \frac{E_1}{1-\nu^2}, A_{12} = \frac{E_1\nu}{1-\nu^2}, A_{66} = \frac{E_1}{2\left(1+\nu\right)}, \\ B_{11} &= B_{22} = \frac{E_2}{1-\nu^2}, B_{12} = \frac{E_2\nu}{1-\nu^2}, B_{66} = \frac{E_2}{2\left(1+\nu\right)}, \\ D_{11} &= D_{22} = \frac{E_3}{1-\nu^2}, D_{12} = \frac{E_3\nu}{1-\nu^2}, D_{66} = \frac{E_3}{2\left(1+\nu\right)}, \end{aligned} \tag{10}$$

with

$$
\begin{aligned}
&E_1 = \left(E_m + \frac{E_c - E_m}{k+1}\right) h, E_2 = \frac{(E_c - E_m)\, kh^2}{2\,(k+1)\,(k+2)},\\
&E_3 = \left[\frac{E_m}{12} + (E_c - E_m)\left(\frac{1}{k+3} - \frac{1}{k+2} + \frac{1}{4k+4}\right)\right] h^3,\\
&I_s = \frac{d_s h_s^3}{12} + A_s z_s^2, I_r = \frac{d_r h_r^3}{12} + A_r z_r^2,\\
&C_s = \pm\frac{E_s A_s z_s}{s_s}, C_r = \pm\frac{E_r A_r z_r}{s_r},\\
&z_s = \frac{h_s + h}{2}, z_r = \frac{h_r + h}{2},
\end{aligned}
\tag{11}
$$

where coupling parameters C_s and C_r are negative for outside stiffeners and positive for inside ones. The spacings of the stringer and ring stiffeners are denoted by s_s and s_r respectively. The quantities A_s, A_r are cross-section areas of stiffeners and I_s, I_r, z_s, z_r are second moments of cross section areas and eccentricities of stiffeners with respect to the middle surface of shell, respectively. The width and thickness of the stringer and ring stiffeners are denoted by d_s, h_s and d_r, h_r respectively. Young modulus of stiffeners E_s, E_r take the values, E_m, if the full metal stiffeners are put at the metal-rich side of the shell and conversely, and E_c, if the full ceramic ones are put at the ceramic-rich side.

From the constitutive relations (8), one can write inversely

$$
\begin{aligned}
&\varepsilon_x^0 = A_{22}^* N_x - A_{12}^* N_y + B_{11}^* \chi_x + B_{12}^* \chi_y,\\
&\varepsilon_y^0 = A_{11}^* N_y - A_{12}^* N_x + B_{21}^* \chi_x + B_{22}^* \chi_y,\\
&\gamma_{xy}^0 = A_{66}^* + 2B_{66}^* \chi_{xy},
\end{aligned}
\tag{12}
$$

in which

$$
\begin{aligned}
&A_{11}^* = \frac{1}{\Delta}\left(A_{11} + \frac{E_s A_s}{s_s}\right), A_{12}^* = \frac{A_{12}}{\Delta}, A_{22}^* = \frac{1}{\Delta}\left(A_{22} + \frac{E_r A_r}{s_r}\right),\\
&A_{66}^* = \frac{1}{A_{66}}, \Delta = \left(A_{11} + \frac{E_s A_s}{s_s}\right)\left(A_{22} + \frac{E_r A_r}{s_r}\right) - A_{12}^2.\\
&B_{11}^* = A_{22}^*\,(B_{11} + C_s) - A_{12}^* B_{12}, B_{22}^* = A_{11}^*\,(B_{22} + C_r) - A_{12}^* B_{12},\\
&B_{12}^* = A_{22}^* B_{12} - A_{12}^*\,(B_{22} + C_r)\,, B_{21}^* = A_{11}^* B_{12} - A_{12}^*\,(B_{11} + C_s)\,,\\
&B_{66}^* = \frac{B_{66}}{A_{66}},
\end{aligned}
\tag{13}
$$

Substituting Eq. (12) into Eq. (9) leads to

$$
\begin{aligned}
&M_x = B_{11}^* N_x + B_{21}^* N_y - D_{11}^* \chi_x - D_{12}^* \chi_y,\\
&M_y = B_{12}^* N_x + B_{22}^* N_y - D_{21}^* \chi_x - D_{22}^* \chi_y,\\
&M_{xy} = B_{66}^* N_{xy} - 2D_{66}^* \chi_{xy},
\end{aligned}
\tag{14}
$$

in which

$$\begin{aligned}
D_{11}^{*} &= D_{11} + \frac{E_s I_s}{s_s} - (B_{11} + C_s) B_{11}^{*} - B_{12} B_{21}^{*}, \\
D_{22}^{*} &= D_{22} + \frac{E_r I_r}{s_r} - B_{12} B_{12}^{*} - (B_{22} + C_r) B_{22}^{*}, \\
D_{12}^{*} &= D_{12} - (B_{11} + C_s) B_{12}^{*} - B_{12} B_{22}^{*}, \\
D_{21}^{*} &= D_{12} - B_{12} B_{11}^{*} - (B_{22} + C_r) B_{21}^{*}, \\
D_{66}^{*} &= D_{66} - B_{66} B_{66}^{*}.
\end{aligned} \tag{15}$$

The nonlinear equations of motion of a cylindrical thin shell based on the classical shell theory and the assumption $u \ll w$ and $v \ll w$, $\rho_1 \dfrac{\partial^2 u}{\partial t^2} \to 0$, $\rho_1 \dfrac{\partial^2 v}{\partial t^2} \to 0$ [14, 15, 44] are given in Refs. [5, 15]

$$\begin{aligned}
&\frac{\partial N_x}{\partial x} + \frac{\partial N_{xy}}{\partial y} = 0, \\
&\frac{\partial N_{xy}}{\partial x} + \frac{\partial N_y}{\partial y} = 0, \\
&\frac{\partial^2 M_x}{\partial x^2} + 2\frac{\partial^2 M_{xy}}{\partial x \partial y} + \frac{\partial^2 M_y}{\partial y^2} + N_x \left(\frac{\partial^2 w}{\partial x^2} + \frac{\partial^2 w_0}{\partial x^2} \right) + 2N_{xy} \left(\frac{\partial^2 w}{\partial x \partial y} + \frac{\partial^2 w_0}{\partial x \partial y} \right) + \\
&\qquad + N_y \left(\frac{\partial^2 w}{\partial y^2} + \frac{\partial^2 w_0}{\partial y^2} \right) + \frac{1}{R} N_y - K_1 w + K_2 \left(\frac{\partial^2 w}{\partial x^2} + \frac{\partial^2 w}{\partial y^2} \right) = \rho_1 \frac{\partial^2 w}{\partial t^2},
\end{aligned} \tag{16}$$

where

$$\rho_1 = \int_{-h/2}^{h/2} \rho(z) \mathrm{d}z + \rho_s \frac{A_s}{s_s} + \rho_r \frac{A_r}{s_r} = \left(\rho_m + \frac{\rho_c - \rho_m}{k+1} \right) h + \rho_s \frac{A_s}{s_s} + \rho_r \frac{A_r}{s_r}, \tag{17}$$

with

$$\begin{aligned}
\rho_s = \rho_m; \rho_r = \rho_m \quad &\text{for metal stiffeners,} \\
\rho_s = \rho_c; \rho_r = \rho_c \quad &\text{for ceramic stiffeners.}
\end{aligned}$$

Considering the first two of Eqs. (16), a stress function φ may be defined as

$$N_x = \frac{\partial^2 \varphi}{\partial y^2}, N_y = \frac{\partial^2 \varphi}{\partial x^2}, N_{xy} = -\frac{\partial^2 \varphi}{\partial x \partial y}. \tag{18}$$

Substituting Eq. (12) into the compatibility Eq. (4) and Eq. (14) into the third of Eq. (16), taking into account Eqs. (2) and (18) neglecting small terms of higher second

order with respect to w_0, yields

$$A_{11}^{*}\frac{\partial^4\varphi}{\partial x^4}+(A_{66}^{*}-2A_{12}^{*})\frac{\partial^4\varphi}{\partial x^2\partial y^2}+A_{22}^{*}\frac{\partial^4\varphi}{\partial y^4}+B_{21}^{*}\frac{\partial^4 w}{\partial x^4}+$$
$$+(B_{11}^{*}+B_{22}^{*}-2B_{66}^{*})\frac{\partial^4 w}{\partial x^2\partial y^2}+B_{12}^{*}\frac{\partial^4 w}{\partial y^4}+\frac{1}{R}\frac{\partial^2 w}{\partial x^2}- \tag{19}$$
$$-\left[\left(\frac{\partial^2 w}{\partial x\partial y}\right)^2-\frac{\partial^2 w}{\partial x^2}\frac{\partial^2 w}{\partial y^2}\right]-2\frac{\partial^2 w}{\partial x\partial y}\frac{\partial^2 w_0}{\partial x\partial y}+\frac{\partial^2 w}{\partial x^2}\frac{\partial^2 w_0}{\partial y^2}+\frac{\partial^2 w}{\partial y^2}\frac{\partial^2 w_0}{\partial x^2}=0,$$

$$\rho_1\frac{\partial^2 w}{\partial t^2}+D_{11}^{*}\frac{\partial^4 w}{\partial x^4}+(D_{12}^{*}+D_{21}^{*}+4D_{66}^{*})\frac{\partial^4 w}{\partial x^2\partial y^2}+D_{22}^{*}\frac{\partial^4 w}{\partial y^4}-B_{21}^{*}\frac{\partial^4\varphi}{\partial x^4}-$$
$$-(B_{11}^{*}+B_{22}^{*}-2B_{66}^{*})\frac{\partial^4\varphi}{\partial x^2\partial y^2}-B_{12}^{*}\frac{\partial^4\varphi}{\partial y^4}-\frac{1}{R}\frac{\partial^2\varphi}{\partial x^2}-\frac{\partial^2\varphi}{\partial y^2}\left(\frac{\partial^2 w}{\partial x^2}+\frac{\partial^2 w_0}{\partial x^2}\right)+$$
$$+2\frac{\partial^2\varphi}{\partial x\partial y}\left(\frac{\partial^2 w}{\partial x\partial y}+\frac{\partial^2 w_0}{\partial x\partial y}\right)-\frac{\partial^2\varphi}{\partial x^2}\left(\frac{\partial^2 w}{\partial y^2}+\frac{\partial^2 w_0}{\partial y^2}\right)+K_1 w-K_2\left(\frac{\partial^2 w}{\partial x^2}+\frac{\partial^2 w}{\partial y^2}\right)=0. \tag{20}$$

Eqs. (19) and (20) are a nonlinear equation system in terms of two dependent unknowns w and φ. They are used to investigate the static and dynamic characteristics of imperfect ES-FGM circular cylindrical shells surrounded by an elastic foundation.

3. NONLINEAR STATIC AND DYNAMIC BUCKLING ANALYSIS

Suppose that an imperfect ES-FGM cylindrical shell surrounded by an elastic foundation is simply supported and subjected to axial compressive load $\bar{r}_0 = r_0 h$ where $r_0 = r_0(t)$ is the average axial stress on the shell's end sections, positive when the shells subjected to axial compression (in $\mathrm{N/m^2}$). Thus, the boundary conditions considered in the current study are

$$w=0,\quad M_x=0,\quad N_x=-r_0 h,\quad N_{xy}=0,\quad \text{at}\quad x=0;L. \tag{21}$$

The deflection of shell is satisfying the mentioned condition (21) is represented by

$$w=f(t)\sin\frac{m\pi x}{L}\sin\frac{ny}{R}, \tag{22}$$

where $f(t)$ is time dependent total amplitude, m is number of half waves in axial direction and n is number of wave in circumferential direction.

The initial-imperfection w_0 is assumed to be the same form of the deflection w as

$$w_0=f_0\sin\frac{m\pi x}{L}\sin\frac{ny}{R}, \tag{23}$$

where f_0 is the known imperfect amplitude.

Substituting Eqs. (22) and (23) into Eq. (19) and solving obtained equation for unknown φ lead to

$$\varphi=\varphi_1\cos\frac{2m\pi x}{L}+\varphi_2\cos\frac{2ny}{R}-\varphi_3\sin\frac{m\pi x}{L}\sin\frac{ny}{R}-r_0 h\frac{y^2}{2}, \tag{24}$$

where denote

$$\begin{aligned}
\varphi_1 &= \frac{n^2\lambda^2}{32m^2\pi^2A_{11}^*} f\left(f+2f_0\right), \\
\varphi_2 &= \frac{m^2\pi^2}{32n^2\lambda^2A_{22}^*} f\left(f+2f_0\right), \\
\varphi_3 &= \frac{\left[B_{21}^* m^4\pi^4 + \left(B_{11}^* + B_{22}^* - 2B_{66}^*\right) m^2n^2\pi^2\lambda^2 + B_{12}^* n^4\lambda^4 - \frac{L^2}{R} m^2\pi^2\right]}{A_{11}^* m^4\pi^4 + \left(A_{66}^* - 2A_{12}^*\right) m^2n^2\pi^2\lambda^2 + A_{22}^* n^4\lambda^4} f, \\
f &= f\left(t\right), \lambda = \frac{L}{R}.
\end{aligned} \tag{25}$$

Substituting the expressions (22-24) into Eq. (20) and applying Galerkin method to the resulting equation yield

$$\begin{aligned}
\rho_1 L^4 \ddot{f} + \left(D + \frac{B^2}{A}\right) f + Gf\left(f+f_0\right)\left(f+2f_0\right) \\
- L^2m^2\pi^2hr_0\left(f+f_0\right) + L^4K_1 f + L^2\left(m^2\pi^2 + n^2\lambda^2\right) K_2 f = 0,
\end{aligned} \tag{26}$$

where

$$\begin{aligned}
A &= A_{11}^* m^4\pi^4 + \left(A_{66}^* - 2A_{12}^*\right) m^2n^2\pi^2\lambda^2 + A_{22}^* n^4\lambda^4, \\
B &= B_{21}^* m^4\pi^4 + \left(B_{11}^* + B_{22}^* - 2B_{66}^*\right) m^2n^2\pi^2\lambda^2 + B_{12}^* n^4\lambda^4 - \frac{L^2}{R} m^2\pi^2, \\
D &= D_{11}^* m^4\pi^4 + \left(D_{12}^* + D_{21}^* + 4D_{66}^*\right) m^2n^2\pi^2\lambda^2 + D_{22}^* n^4\lambda^4, \\
G &= \left(\frac{n^4\lambda^4}{16A_{11}^*} + \frac{m^4\pi^4}{16A_{22}^*}\right).
\end{aligned} \tag{27}$$

Introducing parameters

$$\bar{D} = \frac{D}{h^3}, \bar{B} = \frac{B}{h}, \bar{A} = Ah, \bar{G} = \frac{G}{h}, \xi = \frac{f}{h}, \xi_0 = \frac{f_0}{h}, \tag{28}$$

the non-dimension form of Eq. (26) is written as

$$\begin{aligned}
\frac{\rho_1 L^4}{h^3}\ddot{\xi} + \left(\bar{D} + \frac{\bar{B}^2}{\bar{A}}\right)\xi + \bar{G}\xi\left(\xi+\xi_0\right)\left(\xi+2\xi_0\right) - \\
- \left(\frac{L}{h}\right)^2 m^2\pi^2\left(\xi+\xi_0\right) r_0 + \frac{L^4}{h^3}K_1\xi + \frac{L^2}{h^3}\left(m^2\pi^2 + n^2\lambda^2\right) K_2\xi = 0.
\end{aligned} \tag{29}$$

3.1. Static buckling and post-buckling analysis

Omitting the term of inertia, Eq. (29) leads to

$$r_0 = \frac{h^2}{L^2m^2\pi^2}\left(\bar{D} + \frac{\bar{B}^2}{\bar{A}}\right)\frac{\xi}{\left(\xi+\xi_0\right)} + \frac{L^2K_1 + \left(m^2\pi^2 + n^2\lambda^2\right)K_2}{m^2\pi^2h}\frac{\xi}{\left(\xi+\xi_0\right)} + \frac{h^2}{L^2m^2\pi^2}\bar{G}\xi\left(\xi+2\xi_0\right). \tag{30}$$

Putting $\xi_0 = 0$ in Eq. (30), yields

$$r_0 = \frac{h^2}{L^2 m^2 \pi^2}\left(\bar{D} + \frac{\bar{B}^2}{\bar{A}}\right) + \frac{L^2 K_1 + \left(m^2\pi^2 + n^2\lambda^2\right) K_2}{m^2\pi^2 h} + \frac{h^2}{L^2 m^2 \pi^2}\bar{G}\xi^2. \tag{31}$$

By taking $\xi \to 0$ the buckling stress of perfect ES-FGM cylindrical shells can be determined from Eq. (31)

$$r_{sbu} = \frac{h^2}{L^2 m^2 \pi^2}\left(\bar{D} + \frac{\bar{B}^2}{\bar{A}}\right) + \frac{L^2 K_1 + \left(m^2\pi^2 + n^2\lambda^2\right) K_2}{m^2\pi^2 h}. \tag{32}$$

The static critical buckling stress of perfect ES-FGM cylindrical shells are determined by condition $r_{scr} = \min r_{sbu}$ vs. (m, n) and the static post-buckling curves of perfect and imperfect shells may be traced by using Eqs. (30 and 31) with the same buckling mode shape of critical buckling stress for evaluate static behavior.

3.2. Dynamic buckling analysis

The dynamic buckling analysis will be considered for two load types.

Firstly, the axial compression linearly varying on time $r_0 = ct$ in which c is a loading speed. By using the Runge-Kutta method, the dynamic responses of ES-FGM cylindrical shells can be determined from Eq. (29). The dynamic critical time t_{cr} can be obtained by Budiansky-Roth criterion (Budiansky and Roth [25]): For large value of loading speed, the amplitude-time curve of obtained displacement response increases sharply and this curve obtain a maximum by passing from the slope point and at the corresponding time $t = t_{cr}$ the stability loss occurs. Here, t_{cr} is called critical time and the corresponding dynamic critical buckling stress $r_{dcr} = ct_{cr}$ and dynamic coefficient $\tau_{cr} = \dfrac{r_{dcr}}{r_{scr}}$.

Secondly, the shell is conducted for step loading of infinite duration $r_0 = \text{const}, \forall\, t$. The dynamic critical load is found based on the criterion mentioned by Ganapathi [45]. The load corresponding to a sudden jump in the maximum average deflection in the time history of the shell is taken as the critical buckling step load.

4. NUMERICAL RESULTS

To validate the present approach, two comparisons on critical buckling load are considered. Firstly, Tab. 1 shows the dynamic buckling of perfect un-stiffened FGM cylindrical shells without foundation under linear-time compression, which was also analyzed by Huang and Han [24] by using classical thin shell theory and applying the energy method. Secondly, the present critical static buckling load (see Tab. 2) of stiffened homogeneous cylindrical shells without foundation under axial compression is compared with results in the monograph of Brush and Almroth [42] (based on equations in page 180) where the smeared stiffeners technique, equilibrium path and classical shell theory are used. As can be seen, the very good agreements are obtained in two comparisons.

To illustrate the proposed approach of eccentrically stiffened FGM cylindrical shells surrounded by an elastic foundation, the stiffened and un-stiffened FGM cylindrical shells are considered with $R = 0.5$ m, $L = 0.75$ m, $R/h = 250$. The combination of materials consists of Aluminum $E_m = 7 \times 10^{10}$ N/m^2, $\rho_m = 2702$ kg/m^3 and Alumina $E_c = 38 \times 10^{10}$

N/m^2, $\rho_c = 3800$ kg/m^3. The compressive stress of dynamic analysis is taken to be $r_0 = 10^{10}t$. The Poisson's ratio ν is chosen to be 0.3. The height of stiffeners is equal to 0.005 m, its width 0.002 m. The material properties are $E_s = E_c$ and $E_r = E_c$, $\rho_s = \rho_c$ and $\rho_r = \rho_c$ with internal stringer stiffeners and internal ring stiffeners; $E_s = E_m$, $E_r = E_m$, $\rho_s = \rho_m$ and $\rho_r = \rho_m$ with external stringer stiffeners and external ring stiffeners, respectively. The stiffener system includes 15 ring stiffeners and 63 stringer stiffeners regularly distributed in the axial and circumferential directions, respectively.

Table 1. Comparison of dynamic critical buckling stress r_{dcr} (MPa) and dynamic coefficient $\tau_{cr} = \frac{r_{dcr}}{r_{scr}}$ of perfect un-stiffened FGM cylindrical shells under linear-time compression

	Present		Huang and Han [24]	
	$r_{dcr}\,(m,n)$	$\tau_{cr} = \frac{r_{dcr}}{r_{scr}}$	$r_{dcr}\,(m,n)$	$\tau_{cr} = \frac{r_{dcr}}{r_{scr}}$
$R/h = 500, L/R = 2, c = 100$ MPa/s				
$k = 0.2$	194,94(2,11)	1.030	194,94(2,11)	1.030
$k = 1.0$	169,94(2,11)	1.034	169,94(2,11)	1.034
$k = 5.0$	149,98(2,11)	1.041	150,25(2,11)	1.040
$R/h = 500, L/R = 2, k = 0.5$				
$c = 100$ MPa/s	181,68(2,11)	1.032	181,67(2,11)	1.032
$c = 50$ MPa/s	179,38(2,11)	1.019	179,37(2,11)	1.019
$c = 10$ MPa/s	177,02(2,11)	1.006	177,97(1,8)	1.009
$L/R = 2, k = 0.2, c = 100$ MPa/s				
$R/h = 800$	124,67(2,12)	1.049	124,91(2,12)	1.051
$R/h = 600$	162,18(3,14)	1.026	162,25(3,14)	1.027
$R/h = 400$	239,56(5,15)	1.013	239,18(5,15)	1.011

Table 2. Comparison of static critical buckling load per unit length $\bar{r}_{scr} = r_{scr}h$ ($\times 10^6$ N/m) of perfect stiffened homogeneous cylindrical shells under axial compression

	Present	Brush and Almroth [42]	Difference (%)
50 rings, 50 stringers, $L = 1$ m, $R = 0.5$ m, $E = 7 \times 10^{10}$ N / m^2, $\upsilon = 0.3$, $d_r = d_s = 0.0025$ m, $h_r = h_s = 0.01$ m.			
Internal stiffeners			
$R/h = 100$	3.0725(6,7)	3.0906(6,7)	0.59
$R/h = 200$	1.4147(6,7)	1.4328(6,7)	1.28
$R/h = 500$	0.6924(5,6)	0.7057(5,6)	1.92
External stiffeners			
$R/h = 100$	3,9529(9,3)	3.9551(9,2)	0.06
$R/h = 200$	2.1410(9,4)	2.1469(9,4)	0.28
$R/h = 500$	1.2764(6,6)	1.2897(6,6)	1.04

In Figs. 2-4, the static post-buckling curves of un-stiffened and stiffened shells with elastic foundation are traced by Eqs. (30) and (31) of perfect ($\xi_0 = 0$) and imperfect ($\xi_0 = 0.1$) cases versus three different values of volume fraction index k ($= 0.2, 1, 5$). As can be seen, the post-buckling curves are lower with increasing values of k. Furthermore, the post-buckling curves of imperfect shells are lower than those of perfect shells when deflection is small and post-buckling curves of imperfect shells is higher than that of perfect shells when the deflection is large.

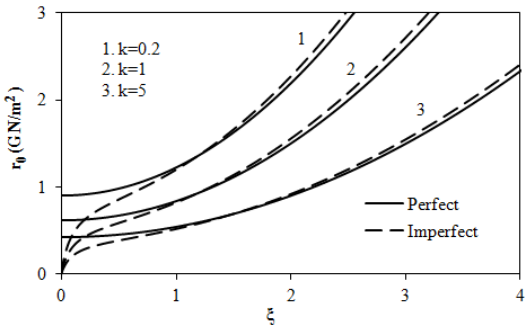

Fig. 2. Effect of k on the static postbuckling of un-stiffened shells ($K_1 = 5 \times 10^8$ N/m^3 and $K_2 = 10^5$ N/m)

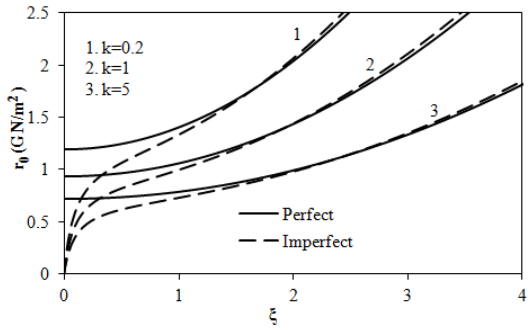

Fig. 3. Effect of k on the static postbuckling of external ring and stringer stiffened shells ($K_1 = 5 \times 10^8$ N/m^3 and $K_2 = 10^5$ N/m)

By using the fourth order Runge-Kutta method, the Eq. (29) is solved to obtain the dynamic responses of perfect ($\xi_0 = 0$) shells under step loading of infinite duration. Dynamic responses of external stiffened shell are presented in Fig. 5. As can be seen, there is a sudden jump in the value of the average deflection when the axial compression reaches the critical value $r_0 = 9,356 \times 10^8$ N/m^2.

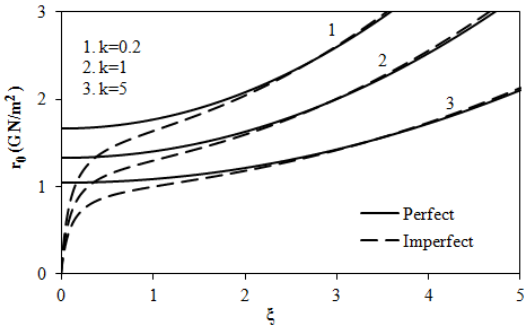

Fig. 4. Effect of k on the static postbuckling of internal ring and stringer stiffened shells ($K_1 = 5 \times 10^8$ N/m^3 and $K_2 = 10^5$ N/m)

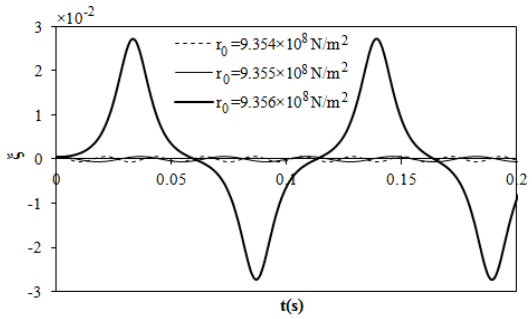

Fig. 5. Dynamic response of external rings and stringers stiffened shell under step loading of infinite duration ($K_1 = 5 \times 10^8$ N/m^3 and $K_2 = 10^5$ N/m)

Figs. 6-8 show the effect of k on the dynamic responses of perfect and imperfect un-stiffened and stiffened shells under linear-time compression. These figures also show

that there is no definite point of instability as in static analysis. Rather, there is a region of instability where the slope of ξ vs t curve increases rapidly for perfect shell. According to the Budiansky-Roth criterion, the critical time t_{cr} can be taken as an intermediate value of this region. This figures also shows that a sudden jump in the value of deflection occurs earlier when k increases and it corresponds a smaller dynamic buckling load.

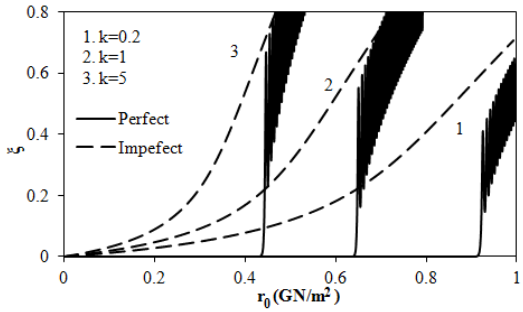

Fig. 6. Effect of k on the dynamic responses of un-stiffened shells under linear-time compression ($K_1 = 5 \times 10^8$ N/m^3 and $K_2 = 10^5$ N/m)

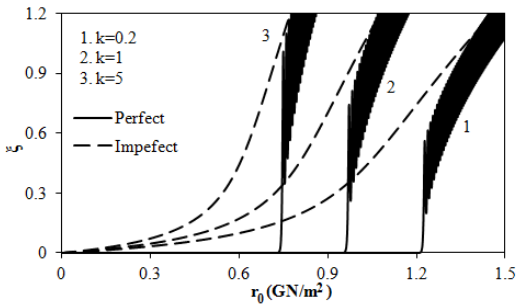

Fig. 7. Effect of k on the dynamic responses of external ring and stringer stiffened shells under linear-time compression ($K_1 = 5 \times 10^8$ N/m^3 and $K_2 = 10^5$ N/m)

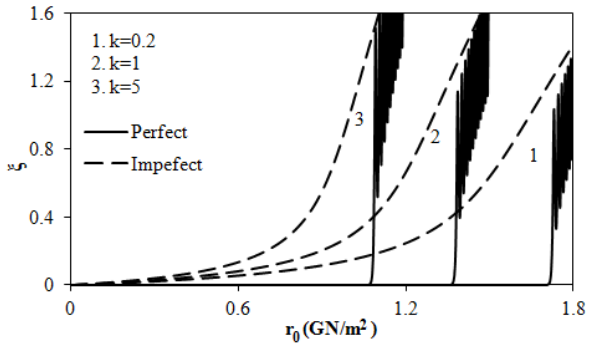

Fig. 8. Effect of k on the dynamic responses of internal ring and stringer stiffened shells under linear-time compression ($K_1 = 5 \times 10^8$ N/m^3 and $K_2 = 10^5$ N/m)

Tab. 3 shows the critical static and dynamic buckling stresses of stiffened and un-stiffened cylindrical shells with elastic foundation ($K_1 = 5 \times 10^8$ N/m^3 and $K_2 = 10^5$ N/m) vs. four different values of volume fraction index $k = (0.2, 1, 5, 10)$. With the same input parameters, the effectiveness of stiffeners are obviously proven; the critical buckling stress of stiffened shell is greater than one of un-stiffened shell. Tab. 3 also shows that the dynamic critical stress decreases with the increase of the volume fraction index k and the buckling modes (m, n) seem smaller for stiffened shells. The critical parameter τ_{cr} is larger than 1, it denotes that the dynamic critical buckling stress of linear time compression case

is larger than static buckling stress. The largest value of and τ_{cr} is equal to 1.072 for the un-stiffened shell with $k = 10$ and the smallest $\tau_{cr} = 1.029$ corresponds to external rings and stringers stiffened shell with $k = 0.2$. The dynamic critical buckling compression of step loading of infinite duration is approximately equal to the static critical buckling compression (like a remark given by Bich et al. [38] for ES-FGM cylindrical shell without foundation).

Table 3. Effect of k on critical static and dynamic buckling stress r_0 ($\times 10^8$ N/m^2)

k	0.2	1	5	10
Unstiffened				
Static	8.968(15,1)	6.153(15,1)	4.175(15,1)	3.776(15,1)
Dynamic $r_0 = \text{const}$	8.968(15,1)	6.154(15,1)	4.175(15,1)	3.776(15,1)
Dynamic $r_0 = ct$	9.242(15,1)	6.494(15,1)	4.447(15,1)	4.049(15,1)
τ_{cr}	1.031	1.055	1.065	1.072
External Rings and Stringers				
Static	11.916(12,6)	9.356(11,9)	7.138(11,3)	6.528(11,1)
Dynamic $r_0 = \text{const}$	11.917(12,6)	9.357(11,9)	7.138(11,3)	6.528(11,1)
Dynamic $r_0 = ct$	12.256(12,6)	9.709(11,9)	7.490(11,3)	6.908(11,1)
τ_{cr}	1.029	1.038	1.049	1.058
Internal Rings and Stringers				
Static	16.696(7,11)	13.331(7,11)	10.414(7,10)	9.831(7,10)
Dynamic $r_0 = \text{const}$	16.696(7,11)	13.332(7,11)	10.415(7,10)	9.831(7,10)
Dynamic $r_0 = ct$	17.259(7,11)	13.830(7,11)	10.904(7,10)	10.323(7,10)
τ_{cr}	1.034	1.037	1.047	1.050

Tab. 4 shows effect of elastic foundation parameters on critical static and dynamic buckling stress for stiffened and un-stiffened shells with and without foundation. Clearly, the critical buckling load of stiffened shells is larger than one of un-stiffened shells and critical buckling load of internal stiffened shells is the largest. In addition, the critical static and dynamic loads of shells increase when the values of foundation parameters K_1 and K_2 increase. It seems that effect of foundation of stiffened shells is larger than one of un-stiffened shells and it attains the largest value with internal stiffened shells.

Effects of the type and position of stiffeners on the nonlinear critical buckling stress of ES-FGM without and with elastic foundation ($K_1 = 5 \times 10^8$ N/m^3 and $K_2 = 10^5$ N/m) are given in Tab. 5. The obtained results show that the ring or stringer stiffeners lightly influence to the critical buckling stress of shells. Conversely, the combination of ring and stringer stiffeners has a considerable effect on the stability of shell. Especially, the critical buckling stress of internal rings and stringers stiffened shell is greatest and the critical buckling stress of internal rings stiffened shell is smallest. For ES-FGM cylindrical shell

with elastic foundation, it seems that effect of stringer stiffeners is more considerable than one of ring stiffeners.

Table 4. Effect of elastic foundation parameters on critical static and dynamic buckling stress r_0 ($\times 10^8$ N/m^2)

K_1	K_2	Un-stiffened		External stiffeners		Internal stiffeners	
(N/m^3)	(N/m)	Static	Dynamic	Static	Dynamic	Static	Dynamic
0	0	4.998(7,15)	5.310(7,15)	7.089(6,13)	7.636(6,13)	8.996(5,11)	9.632(5,11)
5.10^7							
	0	5.071(14,4)	5.368(14,4)	7.385(8,13)	7.850(8,13)	9.512(6,11)	10.096(6,11)
	5.10^4	5.325(14,3)	5.624(14,3)	7.780(8,12)	8.235(8,12)	9.954(6,11)	10.510(6,11)
	10^5	5.576(14,1)	5.860(14,1)	8.138(9,11)	8.553(9,11)	10.395(6,11)	10.953(6,11)
	5.10^5	7.578(14,1)	7.860(14,1)	10.471(11,5)	10.835(11,5)	13.751(6,10)	14.308(6,10)
5.10^8							
	0	5.653(15,1)	5.928(15,1)	8.779(11,9)	9.152(11,9)	12.549(7,11)	13.112(7,11)
	5.10^4	5.703(15,1)	6.175(15,1)	9.067(11,9)	9.424(11,9)	12.940(7,11)	13.383(7,11)
	10^5	6.153(15,1)	6.494(15,1)	9.356(11,9)	9.709(11,9)	13.331(7,11)	13.830(7,11)
	5.10^5	8.155(15,1)	8.431(15,1)	11.389(12,1)	11.756(12,1)	16.276(8,11)	16.726(8,11)
5.10^9							
	0	9.718(20,1)	9.941(20,1)	15.373(16,1)	15.639(16,1)	26.153(12,12)	26.498(12,12)
	5.10^4	9.968(20,1)	10.201(20,1)	15.624(16,1)	15.893(16,1)	26.454(12,11)	26.798(12,11)
	10^5	10.218(20,1)	10.4367(20,1)	15.874(16,1)	16.159(16,1)	26.752(12,11)	27.129(12,11)
	5.10^5	12.219(20,1)	12.437(20,1)	17.876(16,1)	18.158(16,1)	29.135(12,11)	29.467(12,11)

Table 5. Effects of number, type and position of stiffeners on critical static and dynamic buckling stress r_0 ($\times 10^8$ N/m^2)

	Without elastic foundation		With elastic foundation	
	Static	Dynamic ($r_0 = ct$)	Static	Dynamic ($r_0 = ct$)
Unstiffened	4.998(7,15)	5.310(7,15)	6.153(15,1)	6.494(15,1)
ER	5.085(14,1)	5.379(14,1)	6.225(15,1)	6.545(15,1)
IR	5.053(13,10)	5.378(13,10)	6.370(15,8)	6.657(15,8)
ES	5.205(1,8)	7.028(1,8)	9.078(10,12)	9.466(10,12)
IS	5.099(2,10)	6.301(2,10)	11.941(7,15)	12.426(7,15)
IR and IS	8.996(5,11)	9.632(5,11)	13.331(7,11)	13.830(7,11)
ER and ES	7.089(6,13)	7.636(6,13)	9.356(11,9)	9.709(11,9)
IR and ES	7.072(9,11)	7.523(9,11)	9.156(11,10)	9.528(11,10)
ER and IS	7.077(3,11)	7.966(3,11)	12.797(7,13)	13.297(7,13)

where: ER-External rings, IR-Internal rings, ES-External stringers, IS-Internal stringers

Figs. 9-11 show the effects of foundation parameters on the static postbuckling of un-stiffened and stiffened shells. The results show that the postbuckling curves of shell with foundation is upper than one of without foundation shells.

Figs. 12 and 13 show effects of foundation parameters K_1 and K_2 on the static postbuckling of external stiffened shells. These examples show that for various values of K_2, increasing tendency of postbuckling curve is quite similar (Fig. 12). Conversely, the unsimilar tendency is obtained for various values of K_1. There is a small difference between curves as ξ is small. In contrast, this difference becomes considerable when ξ ratio to be larger.

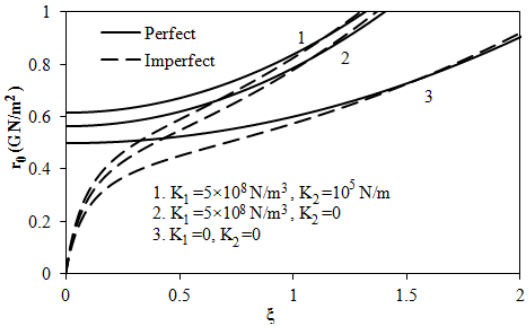

Fig. 9. Effect of foundation on the static postbuckling of un-stiffened FGM cylindrical shell

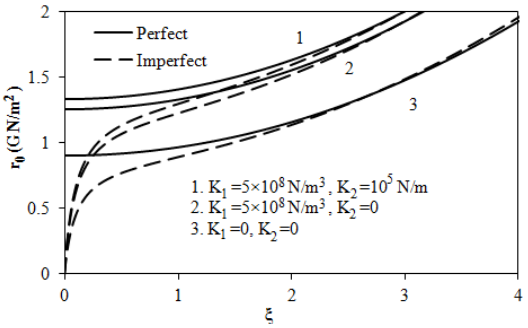

Fig. 10. Effect of foundation on the static postbuckling of internal stiffened FGM cylindrical shell

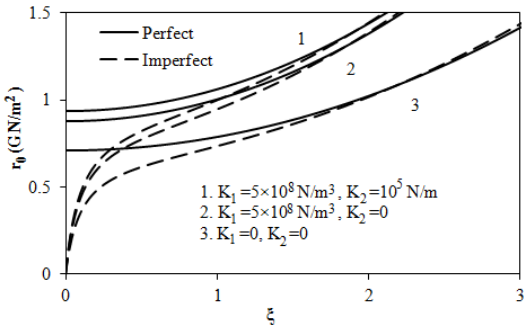

Fig. 11. Effect of foundation on the static postbuckling of external stiffened FGM cylindrical shell

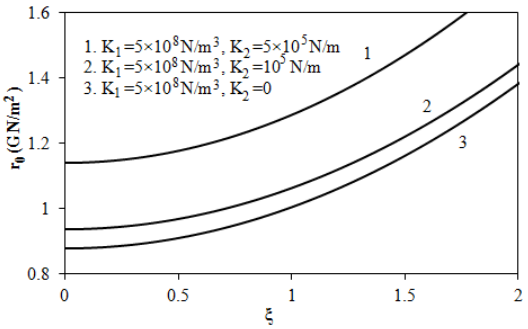

Fig. 12. Effect of foundation parameter K_2 on the static postbuckling of perfect external stiffened FGM cylindrical shell

Figs. 14-16 show effect of foundation on the dynamic response of external stiffened shells. Clearly, the maximal amplitude of dynamic response of instability region of without foundation shell is larger than one of with foundation shell and it decreases when foundation parameters increase.

Finally, Figs. 17 and 18 show effect of foundation parameter K_1 and K_2 on the dynamic response of external stiffened shells. The obtained results show the small difference

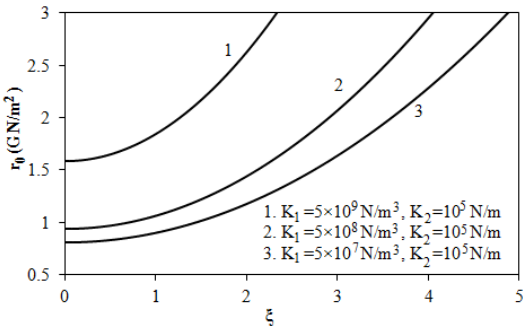

Fig. 13. Effect of foundation parameter K_1 on the static postbuckling of perfect external stiffened FGM cylindrical shell

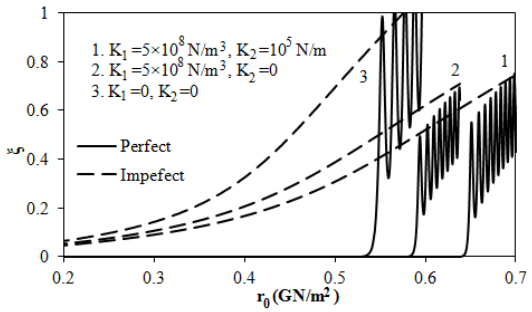

Fig. 14. Effect of foundation on the dynamic response of un-stiffened FGM cylindrical shell

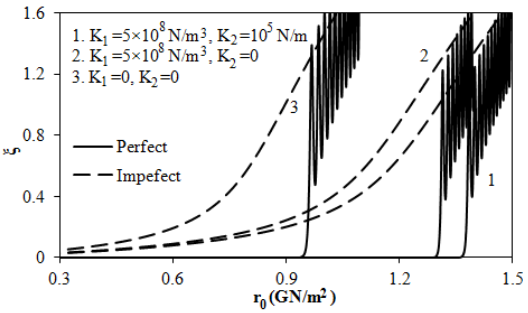

Fig. 15. Effect of foundation on the dynamic response of internal stiffened FGM cylindrical shell

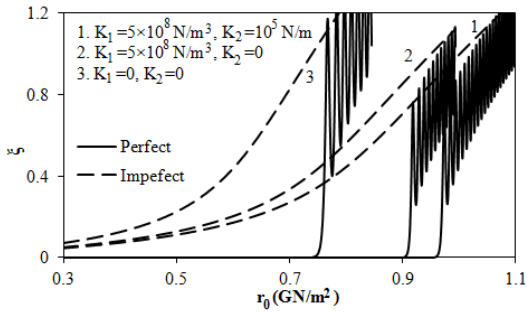

Fig. 16. Effect of foundation on the dynamic response of external stiffened FGM cylindrical shell

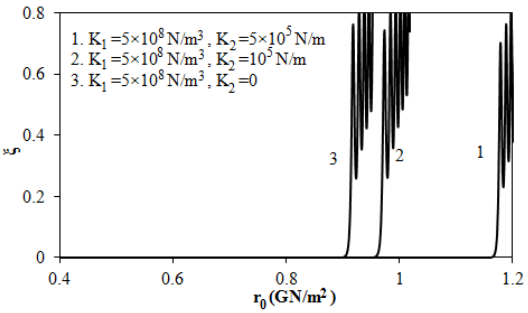

Fig. 17. Effect of foundation parameter K_2 on the dynamic response of perfect external stiffened FGM cylindrical shell

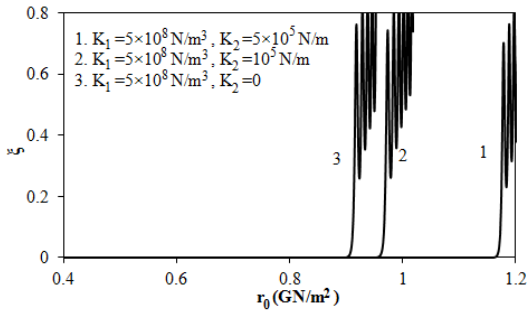

Fig. 18. Effect of foundation parameter K_1 on the dynamic response of perfect external stiffened FGM cylindrical shell

of maximal amplitude of dynamic response of instability region with various value of K_2 (Fig. 17) and the considerable difference is obtained with various value of K_1 (Fig. 18).

5. CONCLUSIONS

This paper presentes an analytical approach on the global buckling and postbuckling behavior of eccentrically stiffened functionally graded circular cylindrical thin shells reinforced by closely spaced stiffener system and surrounded by an elastic foundation based upon the classical shell theory, smeared stiffeners technique with von Karman-Donnell nonlinear terms and two-parameter elastic foundation Pasternak. By using the Galerkin method the explicit expressions of static buckling compression, postbuckling load-deflection curve and nonlinear dynamic equation of ES-FGM circular cylindrical shells are obtained. The later is solved by using the Runge-Kutta method and the criteria for determining critical dynamic compressions are used.

Some conclusions can be obtained:

i). Foundation and stiffeners strongly enhance the static and dynamic stability and load-carrying capacity of FGM cylindrical shells.

ii). Ring stiffeners lightly influence on the stability of shell. But effect of stringer stiffeners is considerable, especially for shell with elastic foundation.

iii). For static postbuckling, the increasing tendency of postbuckling curve is quite similar when K_2 varies. Conversely, the unsimilar tendency is obtained for various values of K_1. For dynamic response, the small difference of maximal amplitude of dynamic response of instability region with various value of K_2 and the considerable difference is obtained with various values of K_1.

ACKNOWLEDGEMENTS

This research is funded by Vietnam National Foundation for Science and Technology Development (NAFOSTED) under grant number 107.02-2013.02.

REFERENCES

[1] H.-S. Shen. Postbuckling analysis of pressure-loaded functionally graded cylindrical shells in thermal environments. *Engineering Structures*, **25**(4), (2003), pp. 487–497.

[2] H.-S. Shen. Thermal postbuckling behavior of functionally graded cylindrical shells with temperature-dependent properties. *International journal of solids and structures*, **41**(7), (2004), pp. 1961–1974.

[3] H.-S. Shen. Postbuckling of axially loaded FGM hybrid cylindrical shells in thermal environments. *Composites science and technology*, **65**(11), (2005), pp. 1675–1690.

[4] H.-S. Shen and N. Noda. Postbuckling of FGM cylindrical shells under combined axial and radial mechanical loads in thermal environments. *International journal of solids and structures*, **42**(16), (2005), pp. 4641–4662.

[5] H. Huang and Q. Han. Buckling of imperfect functionally graded cylindrical shells under axial compression. *European Journal of Mechanics-A/Solids*, **27**(6), (2008), pp. 1026–1036.

[6] H. Huang and Q. Han. Nonlinear elastic buckling and postbuckling of axially compressed functionally graded cylindrical shells. *International Journal of Mechanical Sciences*, **51**(7), (2009), pp. 500–507.

[7] H. Huang and Q. Han. Nonlinear buckling and postbuckling of heated functionally graded cylindrical shells under combined axial compression and radial pressure. *International Journal of Non-Linear Mechanics*, **44**(2), (2009), pp. 209–218.

[8] H. Huang and Q. Han. Research on nonlinear postbuckling of functionally graded cylindrical shells under radial loads. *Composite Structures*, **92**(6), (2010), pp. 1352–1357.

[9] H. Huang and Q. Han. Nonlinear buckling of torsion-loaded functionally graded cylindrical shells in thermal environment. *European Journal of Mechanics-A/Solids*, **29**(1), (2010), pp. 42–48.

[10] H.-S. Shen. Torsional buckling and postbuckling of FGM cylindrical shells in thermal environments. *International Journal of Non-Linear Mechanics*, **44**(6), (2009), pp. 644–657.

[11] A. Sofiyev. Non-linear buckling behavior of FGM truncated conical shells subjected to axial load. *International Journal of Non-Linear Mechanics*, **46**(5), (2011), pp. 711–719.

[12] A. Sofiyev. Influence of the initial imperfection on the non-linear buckling response of FGM truncated conical shells. *International Journal of Mechanical Sciences*, **53**(9), (2011), pp. 753–761.

[13] V. Zozulya and C. Zhang. A high order theory for functionally graded axisymmetric cylindrical shells. *International Journal of Mechanical Sciences*, **60**(1), (2012), pp. 12–22.

[14] M. Darabi, M. Darvizeh, and A. Darvizeh. Non-linear analysis of dynamic stability for functionally graded cylindrical shells under periodic axial loading. *Composite Structures*, **83**(2), (2008), pp. 201–211.

[15] A. Sofiyev and E. Schnack. The stability of functionally graded cylindrical shells under linearly increasing dynamic torsional loading. *Engineering structures*, **26**(10), (2004), pp. 1321–1331.

[16] A. Sofiyev. The stability of compositionally graded ceramic–metal cylindrical shells under aperiodic axial impulsive loading. *Composite structures*, **69**(2), (2005), pp. 247–257.

[17] G. Sheng and X. Wang. Thermomechanical vibration analysis of a functionally graded shell with flowing fluid. *European Journal of Mechanics-A/Solids*, **27**(6), (2008), pp. 1075–1087.

[18] A. Sofiyev. Dynamic buckling of functionally graded cylindrical thin shells under non-periodic impulsive loading. *Acta Mechanica*, **165**(3-4), (2003), pp. 151–163.

[19] A. Sofiyev. The stability of functionally graded truncated conical shells subjected to aperiodic impulsive loading. *International journal of solids and structures*, **41**(13), (2004), pp. 3411–3424.

[20] A. Sofiyev. The vibration and stability behavior of freely supported FGM conical shells subjected to external pressure. *Composite structures*, **89**(3), (2009), pp. 356–366.

[21] A. Sofiyev. The non-linear vibration of FGM truncated conical shells. *Composite Structures*, **94**(7), (2012), pp. 2237–2245.

[22] A. Deniz and A. Sofiyev. The nonlinear dynamic buckling response of functionally graded truncated conical shells. *Journal of sound and vibration*, **332**(4), (2013), pp. 978–992.

[23] C. Hong. Thermal vibration of magnetostrictive functionally graded material shells. *European Journal of Mechanics-A/Solids*, **40**, (2013), pp. 114–122.

[24] H. Huang and Q. Han. Nonlinear dynamic buckling of functionally graded cylindrical shells subjected to time-dependent axial load. *Composite Structures*, **92**(2), (2010), pp. 593–598.

[25] B. Budiansky and R. S. Roth. Axisymmetric dynamic buckling of clamped shallow spherical shells. *NASA technical note D_ 510*, (1962), pp. 597–606.

[26] H.-S. Shen. Postbuckling of shear deformable FGM cylindrical shells surrounded by an elastic medium. *International Journal of Mechanical Sciences*, **51**(5), (2009), pp. 372–383.

[27] H.-S. Shen, J. Yang, and S. Kitipornchai. Postbuckling of internal pressure loaded FGM cylindrical shells surrounded by an elastic medium. *European Journal of Mechanics-A/Solids*, **29**(3), (2010), pp. 448–460.

[28] E. Bagherizadeh, Y. Kiani, and M. Eslami. Mechanical buckling of functionally graded material cylindrical shells surrounded by Pasternak elastic foundation. *Composite Structures*, **93**(11), (2011), pp. 3063–3071.

[29] A. Sofiyev. Buckling analysis of FGM circular shells under combined loads and resting on the Pasternak type elastic foundation. *Mechanics Research Communications*, **37**(6), (2010), pp. 539–544.

[30] A. Najafov, A. Sofiyev, and N. Kuruoglu. Torsional vibration and stability of functionally graded orthotropic cylindrical shells on elastic foundations. *Meccanica*, **48**(4), (2013), pp. 829–840.

[31] A. Sofiyev. Thermal buckling of FGM shells resting on a two-parameter elastic foundation. *Thin-Walled Structures*, **49**(10), (2011), pp. 1304–1311.

[32] A. Najafov and A. Sofiyev. The non-linear dynamics of FGM truncated conical shells surrounded by an elastic medium. *International Journal of Mechanical Sciences*, **66**, (2013), pp. 33–44.

[33] A. Sofiyev and N. Kuruoglu. Non-linear buckling of an FGM truncated conical shell surrounded by an elastic medium. *International Journal of Pressure Vessels and Piping*, **107**, (2013), pp. 38–49.

[34] M. Najafizadeh, A. Hasani, and P. Khazaeinejad. Mechanical stability of functionally graded stiffened cylindrical shells. *Applied Mathematical Modelling*, **33**(2), (2009), pp. 1151–1157.

[35] D. H. Bich, V. H. Nam, and N. T. Phuong. Nonlinear postbuckling of eccentrically stiffened functionally graded plates and shallow shells. *Vietnam Journal of Mechanics*, **33**(3), (2011), pp. 131–147.

[36] D. H. Bich, D. V. Dung, and V. H. Nam. Nonlinear dynamical analysis of eccentrically stiffened functionally graded cylindrical panels. *Composite Structures*, **94**(8), (2012), pp. 2465–2473.

[37] D. H. Bich, D. V. Dung, and V. H. Nam. Nonlinear dynamic analysis of eccentrically stiffened imperfect functionally graded doubly curved thin shallow shells. *Composite Structures*, **96**, (2013), pp. 384–395.

[38] D. H. Bich, D. V. Dung, V. H. Nam, and N. T. Phuong. Nonlinear static and dynamic buckling analysis of imperfect eccentrically stiffened functionally graded circular cylindrical thin shells under axial compression. *International Journal of Mechanical Sciences*, **74**, (2013), pp. 190–200.

[39] D. V. Dung and L. K. Hoa. Nonlinear buckling and post-buckling analysis of eccentrically stiffened functionally graded circular cylindrical shells under external pressure. *Thin-Walled Structures*, **63**, (2013), pp. 117–124.

[40] D. V. Dung and L. K. Hoa. Research on nonlinear torsional buckling and post-buckling of eccentrically stiffened functionally graded thin circular cylindrical shells. *Composites Part B: Engineering*, **51**, (2013), pp. 300–309.

[41] D. V. Dung, L. K. Hoa, N. T. Nga, and L. T. N. Anh. Instability of eccentrically stiffened functionally graded truncated conical shells under mechanical loads. *Composite Structures*, **106**, (2013), pp. 104–113.

[42] D. O. Brush and B. O. Almroth. *Buckling of bars, plates, and shells*, Vol. 6. McGraw-Hill New York, (1975).

[43] J. N. Reddy and J. H. Starnes. General buckling of stiffened circular cylindrical shells according to a layerwise theory. *Computers & structures*, **49**(4), (1993), pp. 605–616.

[44] A. Volmir. *Non-linear dynamics of plates and shells*. Science Edition M, (1972). (in Russian)

[45] M. Ganapathi. Dynamic stability characteristics of functionally graded materials shallow spherical shells. *Composite structures*, **79**(3), (2007), pp. 338–343.

VIETNAM ACADEMY OF SCIENCE AND TECHNOLOGY
VIETNAM JOURNAL OF MECHANICS VOLUME 36, N. 1, 2014

CONTENTS

Pages

1. Nguyen Van Khang, Tran Ngoc An, Crack detection of a beam-like bridge using 3D mode shapes 1
2. Nguyen Viet Khoa, Crack detection of a beam-like bridge using 3D mode shapes. 13
3. Vu Hoai Nam, Nguyen Thi Phuong, Dao Huy Bich, Dao Van Dung, Nonlinear static and dynamic buckling of eccentrically stiffened functionally graded cylindrical shells under axial compression surrounded by an elastic foundation. 27
4. Nguyen Xuan Toan, Dynamic interaction between the two-axle vehicle and continuous girder bridge with considering vehicle braking force. 49
5. Nguyen Thoi Trung, Phung Van Phuc, Tran Viet Anh, Nguyen Tran Chan, Dynamic analysis of Mindlin plates on viscoelastic foundations under a moving vehicle by CS-MIN3 based on C^0-type higher-order shear deformation theory. 61